Dalton Transactions

Accepted Manuscript

ROYAL SOCIETY OF CHEMISTRY

www.rsc.org/dalton

Cite this: DOI: 10.1039/c0xx00000x

www.rsc.org/xxxxxx

ARTICLE TYPE

Incorporation of imidazole within the metal-organic framework UiO-67 for enhanced anhydrous proton conductivity

Shucheng Liu, Zifeng Yue, and Yi Liu*

Received (in XXX, XXX) Xth XXXXXXXXX 20XX, Accepted Xth XXXXXXXXX 20XX

DOI: 10.1039/b000000x

Iimidazole was introduced into the channels of the metal-organic framework UiO-67 using an evaporation method. The imidazole@UiO-67 composite presents a high proton conductivity of 1.44×10^{-3} Scm^{-1} at 120℃ under anhydrous conditions. With a low activation energy at high temperatures (0.36 eV), the hybrid material can be regarded as a super-ionic conductor.

Proton-conducting materials are an important component of fuel cells. The first proton-conducting material used as a fuel cell separator/proton conductor was the perfluorinated sulfonated polymer commercially known as Nafion, which operates in a temperature range of 20-80°C with a high conductivity (10^{-2} Scm^{-1})[1]. Nafion and similar polymeric materials have been widely used in fuel cells operating at low temperature; however, the conductivity of these sulfonated polymers decreases significantly above 80 °C due to the loss of chemically-bound water. Development of new conducting materials with higher proton conductivity that undergoes anhydrous conditions is required to increase the efficiency of fuel cells.

One approach for developing ion conducting separators that operate at higher temperatures, is to load guest molecule (protic molecules or ions) into the pores of solid supports, such as porous materials [2-8]. Heteropolyacids as composite membranes on silica supports [9] and perfluoroalkylsulfonic acid grafted on the surface of mesoporous silica [10] have been studied. Such composite solids show proton conductivity values (0.1 Scm^{-1}) comparable to that of Nafion. The proton conductivity, however, drops substantially at temperatures above 80 °C, similar to Nafion.

Metal-organic frameworks (MOFs) are a class of hybrid inorganic-organic compounds consisting of networks of metal ions or metal clusters connected via organic ligands [11-14]. This new type of mesoporous functional materials has pores that are adjustable. The structural characteristics of MOFs make them promising for the design of new ion conductors. The comparable sizes of the MOF pore diameters and guest molecules enable the enhancement of the mobility of the guest molecules and ions. S. Kitagawa and co-workers [2,3] have focused on the hybridization of the proton carrier and MOFs on the molecular scale. These authors prepared two imidazole-loaded MOFs and investigated their proton-conduction behavior. Imidazole was loaded into two Al-based frameworks, $[Al(OH)(ndc)]_n$(ndc=1,4-naphthalenedicarboxylate) and $[Al(OH)(bdc)]_n$(bdc=1,4-benzenedicarboxylate). Imidazole@$[Al(OH)(ndc)]_n$ which exhibited an ionic conductivity of 2.2×10^{-5} Scm^{-1} at 120 °C. Imidazole@$[Al(OH)(bdc)]_n$ exhibited a conductivity 1.0×10^{-7} Scm^{-1} at 120 °C. In addition, the composite $[Al(OH)(ndc)]_n$ and histamine was also fabricated, which achieved a conductivity of 1.7×10^{-3} Scm^{-1} at 150 °C in a completely anhydrous environment. The results of these studies demonstrated that proton-conducting

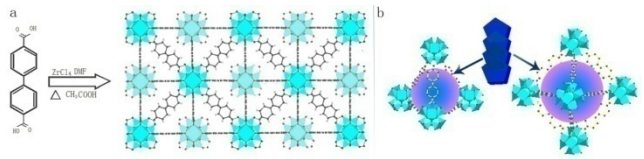

Scheme 1 (a) Schematic representation of formation of UiO- 67 with acetic acid as the modulator. (b) A process of imidazole molecule loading in the channels of UiO-67 (blue is imidazole molecule).

materials incorporated in MOFs show unique proton-conduction behavior resulting from the confinement within the MOFs. The design flexibility and framework tunability of this class of materials suggest that they can serve as a versatile platform for new types of proton conducting materials. Despite the recent progress in hybrid proton conducting MOFs, many challenges remain. The conductivities of the reported guests-loaded proton-conducting MOF materials were insufficient to warrant use of these materials in practical applications. Consequently, further improvement of the basic concept is needed to identify better MOFs supports that are suitable proton carriers.

The UiO-type MOFs (UiO stands for University of Oslo) [15-22], are composed of $\{Zr_6O_4(OH)_4\}$ oxoclusters nodes and dicarboxylate linkers and are known for the excellent thermal and chemical stabilities. The first members of this class were the series UiO-66 (with terephthalate as linker), UiO-67 (with biphenyldicarboxylate) and UiO-68 (with terphenyl dicarboxylate). The thermal stability together with the versatile organic composition and low toxicity of zirconium, make these materials an interesting candidate for use as porous solid supports. However, the incorporation of guest molecules within the pores of UiO-type MOFs has only been recently studied and, to the best of our knowledge, there have been no reports of the synthesis of imidazole@UiO composites. In the work reported herein, imidazole was introduced into the UiO-67 pores to form anhydrous proton carrier pathways. The composite imidazole@UiO-67 achieved a conductivity of more than 10^{-3}

Scm^{-1} at 120 °C in a completely anhydrous environment, which is higher than other imidazole-impregnated MOFs reported to date.

The UiO-67 crystal was synthesized by reacting zirconium chloride ($ZrCl_4$) with 4,4'-Biphenyl dicarboxylic acid (H_2BPDC) modulated by the addition of acetic acid (Scheme 1a). Imidazole molecules were introduced into the pores of UiO-67 using an evaporation method (SI). In order to investigate the concentrations of imidazole in the composites, the different weight ratio of imidazole and UiO-67 were used in process of evaporation. The composite with full imidazole loading is designated imidazole@UiO-67 in this work.

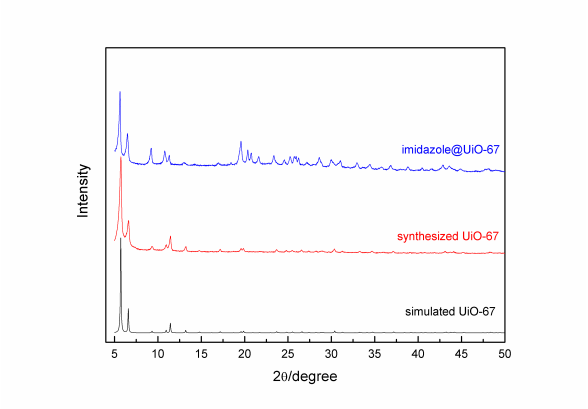

Fig. 1 XRD patterns of UiO-67 and imidazole@UiO-67

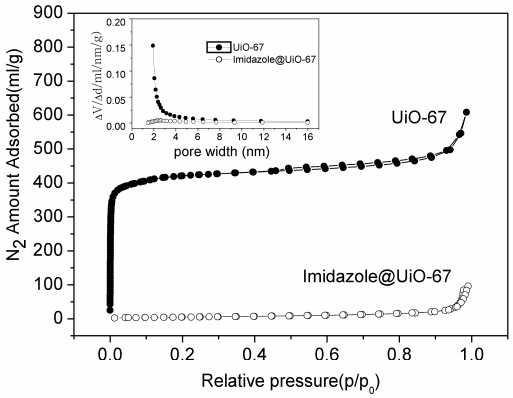

Fig. 2 N_2 adsorption isotherms of UiO-67 and imidazole@UiO-67 at 77K. The insets show the BJH pore size distribution curve.

The crystal structures of UiO-67 and imidazole@UiO-67 were measured using wide-angle X-ray diffraction (XRD) as shown in Fig. 1. The relative intensity and peak positions found in the XRD pattern is consistent with previous reports and theoretical powder patterns [18,22], confirming the formation of the desirable UiO-67 type crystalline frameworks. The UiO-67 crystal is based on the $Zr_6O_4(OH)_4$ building unit, forming lattices by a 12-fold connection through the BPDC linkers, resulting in a face centred cubic (fcc) structure (a=27.1 Å). The structure of the UiO-67 contains two types of cages: an octahedral cage (Scheme 1b, large purple spheres, Φ~18 Å) that is face sharing with 8 tetrahedral cages (Scheme 1b, small purple spheres, Φ~11.5 Å) [16,18]. Powder X-ray diffraction patterns of imidazole@UiO-67 suggested that the framework of UiO-67 was maintained without damage. Moreover, a slight change in Bragg peaks intensity at low angle was noticed that can be associated to the presence of imidazole molecules within the pores of UiO-67.

The N_2 adsorption-desorption isotherm and the Barrett-Joyner-Halenda (BJH) adsorption pore size distribution plot of the composites are shown in Fig. 2. The curves of as synthesized UiO-67 adhere to the type-I isotherm, a typical characteristic of microporous adsorbents. The specific BET surface area of UiO-67 was measured as 1662 m^2g^{-1} (Langmuir surface area is 1892 m^2g^{-1}). The pore size distribution curve of UiO-67 using the BJH model exhibited micropores centered at 1.99 nm with the total pore volume 0.94 cm^3/g. N_2 adsorption of imidazole@UiO-67 at 77K was measured and the adsorbed amount decreased compared with UiO-67, which suggested that imidazole molecules occupied the micropore spaces of UiO-67. The specific BET surface area and the total pore volume of imidazole@UiO-67 was decreased to 18 m^2g^{-1} and 0.15 cm^3/g due to the imidazole loading.

The morphology and microstructure of the samples were examined using TEM. As shown in Fig. 3, the UiO-67 crystal exhibits a tetragonal morphology. The crystal morphology of imidazole@UiO-67 is similar to the UiO-67 crystal, which indicated that the imidazole molecules in the composite were accommodated inside the micropores of UiO-67, not aggregated on the outer surface.

The chemical state of samples was investigated using X-ray photoelectron spectroscopy (XPS) to probe the properties of the inner-shell electrons (Fig.S1). High-resolution narrow-scan spectra were obtained for the O1s, C1s, and Zr3d core levels of UiO-67. The O1s spectrum reveals a component with binding energy (BE) 531.68 eV corresponding to oxygen ions of hydroxyl groups [23]. The two peaks at 182.48 and 184.78eV in the Zr3d spectrum can be ascribed to the spin-orbit splitting of the Zr3d components, Zr3d5/2 and Zr3d3/2. The observed Zr 3d5/2 binding energy of ~182.48 eV for the samples are higher than that of metallic Zr (178.7-180.0 eV), ZrC (178.6−179.6 eV), but comparable to that of hydroxide state Zr^{4+}(OH) (~182.6 eV) [23-25].Therefore, it can be concluded that the Zr atoms are primarily coordinated with oxo and hydroxo oxygen atoms in the composites. When imidazole loading, no obvious BE shifts were observed. The N1s spectrum of imidazole@UiO-67 reveals only one peak at 400.6 eV, which can be attributed to the aromatic heterocyclic structure of imidazole. The XPS results indicated that there is no obvious interaction between imidazoles and carboxylate groups of UiO-67.

The amount of imidazole in UiO-67 was checked by thermogravimetric analysis (TGA) measurement (Fig. 4). TGA of the UiO-67 shows two steps of weight loss. The first step of 10% weight loss (30-300 °C) can be assigned to the loss of water and solvent from the product. The curve shows a stability plateau in the range of 300-500 °C before a second step of an additional 37% weight loss occurs (500-600 °C), which corresponds to the thermal decomposition of the MOF framework. The TGA profile of imidazole@UiO-67 exhibits no weight drop until 140 °C, indicating that the imidazole molecule is accommodated in the pores, not aggregated on the outer surface of the UiO-67 bulk, because the melting temperature of pure imidazole is 93 °C. Above 140°C, there was a 36% the weight loss until the sample

reached 250°C, which was attributed to the release of imidazole from the UiO-67 channels. This would indicate that the UiO-67 absorbed 36% of its weight in imidazole with full loading. The remaining 22% of the composite sample weight loss occurred at the same temperature as the unloaded UiO-67, indicating that the loading and release of imidazole in the pores did not damage the framework of the UiO-67. Considering that the dispersion of imidazole is uniform in the pores of UiO-67, the density of imidazole loaded into the pores can be calculated from the total pore volume of the UiO-67 host. This value is 0.38 g/cm^3, which is lower than the 1.23 g/cm^3 for the bulk imidazole solid [26]. This indicates that the absorbed imidazole molecules in the UiO-67 framework have a different packing arrangement than bulk imidazole. In addition, the content of imidazole in the composites can be controlled by using different weight ratio of imidazole and UiO-67 in process of evaporation. The composites with less content (30% and 21% quantity of imidazole) were obtained (Fig. S2).

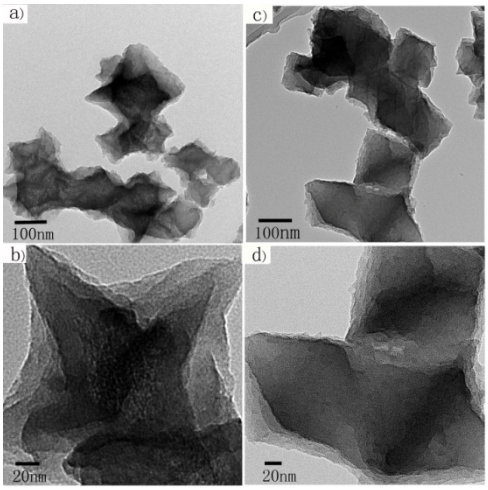

Fig. 3 TEM image of UiO-67(a,b) and Imidazole @UiO-67 (c,d)

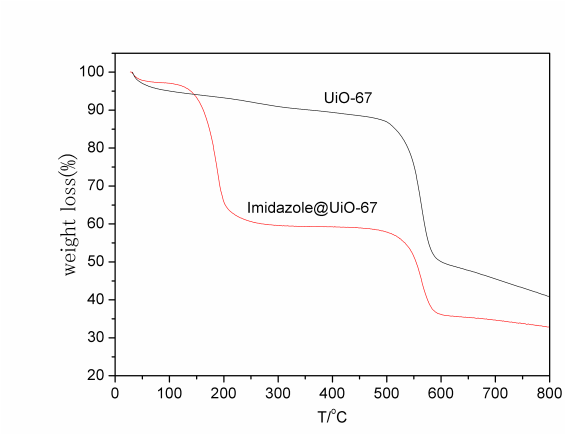

Fig. 4 TGA of UiO-67 and Imidazole@UiO-67 under N_2 atmosphere

The proton conductivity of imidazole confined in the channels of UiO-67 was measured using AC impedance spectroscopy under anhydrous conditions. Samples for conductivity measurements were prepared by pelletizing the Imidazole@UiO-67 composite powders. Below 70°C, the complex-impedance plane plots exhibit only one depressed semi-circular arc at high frequency including the relaxation of protons at the grain interior and grain boundary, as shown in Fig .4. The grain interior and grain boundary arc cannot be separated because the values of the time constant τ of two components are comparable. As a result, it is difficult to separate the grain interior and grain boundary resistances and only the total resistance can be obtained. The resulting equivalent circuit (RC parallel circuit) is adaptable for this case (where R is the total resistance of proton transfer, C is the capacitance). The corresponding capacitance is on the order of 10^{-10} F and varies little with temperature. The Gradual disappearance of the semicircle was observed from 80 to 130 °C due to a decrease in the value of the time constant τ [3].

The conductivity of the samples was calculated using the following equation: σ=L/RS, where L is the thickness of the sample under study, R is the total resistance determined from the fitting of the impedance diagrams, and S is its geometric area. We observed a linear increase in conductivity with increasing temperature: 1.81×10^{-7} Scm^{-1} at 50°C to 1.44×10^{-3} Scm^{-1} at 120℃ and the highest conductivity of 1.52×10^{-3} Scm^{-1} was attained at 130℃. Above 130℃, the conductivity decreased gradually due to the release of imidazole from pores of UiO-67. These results show that the conductivity of the composite at 120 ℃is much higher than that of imidazole@$[Al(OH)(ndc)]_n$ (2.2×10^{-5} Scm^{-1}) and is comparable to the histamine@$[Al(OH)(ndc)]_n$ at 150℃ (1.7×10^{-3} Scm^{-1})[2,3]. It is well known that imidazole exists in two tautomeric forms as a result of the migration of the proton between the two nitrogen atoms, thus providing a pathway for proton conduction. However, the bulk imidazole does not exhibit significant proton conduction exhibiting a conductivity of about 10^{-8} Scm^{-1} at room temperature due to the dense packing of imidazole. Moreover, no detected signal was observed in UiO-67 by the AC impedance spectroscopy in the temperature range measured, which is indicative of negligible proton conductivity for this parent framework. This means a significant improvement in the conductivity arises from the imidazole accommodated by the UiO-67. This incorporation of imidazole into the channels of UiO-67 promotes the dynamic motion of guest molecules, resulting in high proton conduction. It has been reported that this ionic conductivity can be enhanced when a thickness space-charge layers is comparable to the Debye length [27]. The size and shape of imidazole (4.3 Å×3.7 Å) can fit into the tetrahedral cages (Φ~11.5 Å) and octahedral cage (Φ~18 Å) of UiO-67. The flips of confined imidazole within the channel of UiO-67 lead to disruption and rearrangement of the hydrogen bonds which provides more pathways for proton migration, thereby improving proton conduction.

The conductivity as a function of temperature is derived from the Arrhenius equation, expressed as follows:

$$\sigma = \frac{\sigma_0}{T}\exp -\frac{E_a}{kT}$$

Where σ is the ionic conductivity, σ_0 is the pre-exponential factor, T is the absolute temperature, k is the Boltzmann constant and E_a is the activation energy of the proton hopping. Fig. 5d shows the composite conductivity plotted according to the Arrhenius law. The activation energies can be determined from

this Arrhenius curve. It is noteworthy that a change in the activation energy is seen observed near 90 °C. At temperatures ranging from 45 to

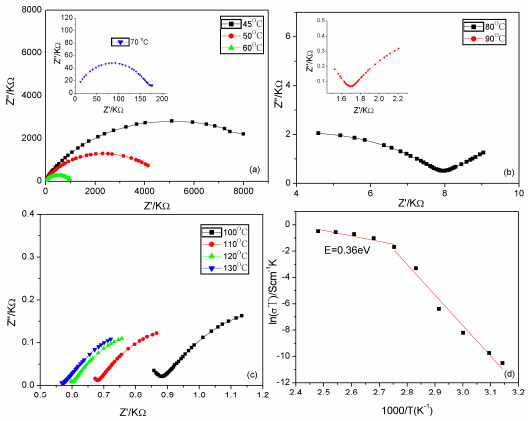

Fig. 5 AC impedance spectra (a-c) and Arrhenius curves (d) of imidazole @UiO-67

90 °C, the composite shows the high activation energy for proton hopping. The activation energy was reduced to 0.36 eV as the temperature increased due to the low interaction between the guest and host and allows the imidazole to pass freely through the host. The low activation energy at high temperature reflects the Grotthuss mechanism of proton conduction for the composite [28,29]. When we introduced a comparatively small amount of imidazole into UiO-67, composites containing 21% quantity of imidazole was obtained. The conductivities were 3.82×10^{-6} Scm^{-1} at 120 ^{o}C, which were three orders of magnitude smaller than that of imidazole@UiO-67 with full loading. The results suggest that the concentration of the proton carrier is critical for conductivity.

To investigate the stability of imidazole inside the cavities of UiO-67, the leaching test on the imidazole@UiO-67 was performed in water (SI). It was found that the imidazole@UiO-67 shows significant structural breakdown after treated with water for 1 hour, as evidenced by the XRD patterns (Fig. S7). AC impedance measurements show that the resistance of the sample is too high, and the AC impedance spectrum could not be obtained in the temperature range measured under anhydrous conditions, which is indicative of negligible proton conductivity for the sample. The results indicate that the imidazole in UiO-67 is not stable and the UiO-67 frameworks are susceptible to degradation by water. The stability test demonstrates that there is limited operation temperature window for the UiO-67 based membranes for fuel cell application as water is the product of the fuel cell reaction. Nevertheless, we think that the hybrid material can be regarded as a super-ionic conductor due to its high conductivity under anhydrous conditions. In the next work, it will be necessary for study of the structural and conductivity stability of the sample under different humidity conditions.

In summary, incorporation of imidazole into the pores of the Zr based MOFs UiO-67 have been successfully executed for the first time, using an evaporation method. The resulting composite achieved a conductivity of over 10^{-3} Scm^{-1} at 120 ^{o}C in a completely anhydrous environment, which is higher than other imidazole-impregnated MOFs reported to date. The UiO-67 host has micropores that are larger enough to accommodate the imidazole guests and facilitate higher mobility, which resulted in the high proton conductivity. With a low activation energy (0.36 eV), it is expected that this new proton-conduction material will offer new opportunities for super-ionic conductors.

Acknowledgements

This work was supported by the National Natural Science Foundation of China (21261006), Natural Science Foundation of Guizhou province (2012/2115) and Graduate Innovation Fund of Guizhou University (2014069).

Notes and references

College of Science, Guizhou University, Guiyang 550025, China
E-mail: sci.yiliu@gzu.edu.cn

† Electronic Supplementary Information (ESI) available: [details of any supplementary information available should be included here]. See DOI: 10.1039/b000000x/

1 S. Paddison, *J. Annu. Rev. Mater. Res.*, 2003, **33**, 289.
2 S.Bureekaew, S.Horike, M.Higuchi, M.Mizuno, T.Kawamura, D.Tanaka, N.Yanai and S.Kitagawa, *Nat. Mater.*, 2009, **8**,831.
3 D.Umeyama, S.Horike, M.Inukai, Y.Hijikata and S.Kitagawa, *Angew. Chem., Int. Ed.*, 2011, **50**, 11706.
4 M.Inukai, S.Horike, D.Umeyama, Y.Hijikatab and S.Kitagawa, *Dalton Trans.*, 2012, **41**,13261.
5 J. A. Hurd, R. Vaidhyanathan, V. Thangadurai, C. I. Ratcliffe,I. L. Moudrakovski and G. K. H. Shimizu, *Nat. Chem.*, 2009, **1**, 705.
6 V. G.Ponomareva, K.A.Kovalenko, A. P.Chupakhin, D.N.Dybtsev, E.S.Shutova and V.P. Fedin, *J. Am. Chem. Soc.*, 2012, **134**, 15640.
7 V. G.Ponomareva, K. A.Kovalenko, A. P.Chupakhin, E. S.Shutova and V.P.Fedin, *Solid. Stat. Ionic.*, 2012, **225**, 420.
8W.Salomon, C.R.Marchal, P.Mialane, P.Rouschmeyer, C.Serre, M. Haouas, F.Taulelle, S.Yang, L.Ruhlmannb and A.Dolbecq , *Chem. Commun.*, 2015, **51**, 2972.
9 N. Azuma, R. Ohtsuka, Y. Morioka, H. Kosugi and J. Kobayashi, *J. Mater. Chem.* 1991, **1**, 989.
10 Y.F.Lin, C.Y.Yen, C.CM. Ma, S.H.Liao,C.H.Lee, Y.H.Hsiao and H.P. Lin, *J. Power. Sources*, 2007,**171**, 388.
11 H.C.Zhou and S.Kitagawa, *Chem. Soc. Rev.*, 2014,**43**, 5415.
12 H.Li, M.Eddaoudi and M.O'Keeff, *Nature*,1999,**402**,276.
13 K.L.Mulfort and J.T.Hupp, *J .Am .Chem. Soc.*, 2007,129,9604.
14 N. Stock and S.Biswas, *Chem. Rev.*, 2012,**112**,933.
15 S.Chavan, J.G.Vitillo, D.Gianolio,O.Zavorotynska,B.Civalleri, S.Jakobsen, M.H. Nilsen,L.Valenzano,C.Lamberti, K. P.Lillerud and S. Bordiga，*Phys. Chem. Chem. Phys.*, 2012, **14**, 1614.
16 M.J. Katz, Z.J.Brown, Y.J. Colón, P.W. Siu, K. A. Scheidt, R.Q. Snurr, J.T. Hupp and O.K. Farha, *Chem. Commun.*, 2013,**49**, 9449 .
17 P.W. Siu, Z.J. Brown,O.K. Farha, J.T. Hupp and K.A. Scheidt, *Chem. Commun.*, 2013,**49**, 10920.
18 J.H.Cavka, S.Jakobsen,U.Olsbye, N.Guillou, C.Lamberti,S.Bordiga and K.P. Lillerud, *J. Am. Chem. Soc.*, 2008,1**30**, 13850.
19 H.Wu, Y.S.Chua, V.Krungleviciute, M.Tyagi, P.Chen,T.Yildirim and W.Zhou, *J. Am. Chem. Soc.*, 2013,**135**, 10525.
20 M.Kandiah, M.H.Nilsen, S.Usseglio, S.Jakobsen,U.Olsbye, M.Tilset, C.Larabi, E.A. Quadrelli,F.Bonino and K. P. Lillerud, *Chem. Mater.*, 2010,**22**, 6632.
21 C.H.Lau, R.Babarao and M.R. Hill, *Chem. Commun.*, 2013,**49**, 3634.
22N.Ko, J.Hong, S.Sung, K.E.Cordova, H.J.Park, J.K.Yang and J. Kim, *Dalton Trans.*, 2015, **44**,2047.
23 I.A.Yashchishuyn, A.M.Korduban, V.V.Trachevskiy, T.E.Konstantinova, I.A.Danilenko, G.K.Volkova and I.K.Nosolev, *Functional Mater,*2010,**17**,306.
24 Y. M.Wang, Y.S.Li, P.C.Wong and K.A.R.Mitchell, *Appl. Surf.Sci*, 1993, **72**, 237.
25 T.L.Barr, *J Phys Chem B*, 1978, **82**, 1801.

26 B. M.Craven, R. K.McMullan, J. D.Bell and H. C.Freeman, *Acta Crystallogr., Sect. B,* 1977, **33**, 2585.
27 T.Yamada, M.Sadakiyo and H. Kitagawa, *J. Am. Chem. Soc.*, 2009, **131**, 3144
28 A.Shigematsu, T.Yamada and H.Kitagawa, *J. Am. Chem. Soc.*, 2011, **133**, 2034.
29 P.Colomban, *Chemistry of Solid State Materials*, Vol. 2, Cambridge University Press: Cambridge, U.K., 1992.